available at www.sciencedirect.com

ScienceDirect

journal homepage: www.ejconline.com

Inhibition profiles of phosphatidylinositol 3-kinase inhibitors against PI3K superfamily and human cancer cell line panel JFCR39

Dexin Kong, Shingo Dan, Kanami Yamazaki, Takao Yamori *

Division of Molecular Pharmacology, Cancer Chemotherapy Center, Japanese Foundation for Cancer Research, 3-10-6, Ariake, Koto-ku, Tokyo 135-8550, Japan

ARTICLE INFO

Article history:
Received 2 November 2009
Received in revised form 18 December 2009
Accepted 6 January 2010
Available online 1 February 2010

Keywords:
Phosphatidylinositol 3-kinase inhibitor
Molecular target
Specificity
JFCR39
ZSTK474

ABSTRACT

As accumulating evidences suggest close involvement of phosphatidylinositol 3-kinase (PI3K) in various diseases particularly cancer, considerable competition occurs in development of PI3K inhibitors. Consequently, novel PI3K inhibitors such as ZSTK474, GDC-0941 and NVP-BEZ235 have been developed. Even though all these inhibitors were reported to inhibit class I PI3K but not dozens of protein kinases, whether they have different molecular targets remained unknown. To investigate such molecular target specificity, we have determined the inhibitory effects of these novel inhibitors together with classical PI3K inhibitor LY294002 on PI3K superfamily (including classes I, II, and III PI3Ks, PI4K and PI3K-related kinases) by using several novel non-radioactive biochemical assays. As a result, ZSTK474 and GDC-0941 indicated highly similar inhibition profiles for PI3K superfamily, with class I PI3K specificity much higher than NVP-BEZ235 and LY294002. We further investigated their growth inhibition effects on JFCR39, a human cancer cell line panel which we established for molecular target identification, and analysed their cell growth inhibition profiles (fingerprints) by using COMPARE analysis programme. Interestingly, we found ZSTK474 exhibited a highly similar fingerprint with GDC-0941 ($r = 0.863$), more similar than with that of either NVP-BEZ235 or LY294002, suggesting that ZSTK474 shares more in molecular targets with GDC-0941 than with either of the other two PI3K inhibitors, consistent with the biochemical assay result. The biological implication of the difference in molecular target specificity of these PI3K inhibitors is under investigation.

1. Introduction

JFCR39 anticancer drug screening system is an informatic drug-activity database that we established previously by exploiting a panel of 39 human cancer cell lines.[1–4] With the use of this system, action mechanism of a test compound can be predicted by comparing its growth inhibition profiles (fingerprint) across the panel of cells with those of the standard anticancer drugs using the COMPARE algorithm.[1,2] So far, utilising this method we have succeeded in predicting the action mechanisms of MS-247 (topoisomerase inhibitor), FJ5002 (telomerase inhibitor), ZSTK474 (Fig. 1) and other compounds.[2,5,6] ZSTK474 was identified as a phosphatidylinositol 3-kinase (PI3K) inhibitor based on the similarity of its fingerprint with that of the well-known PI3K inhibitor LY294002 followed by its biochemical characterisation.[6,7]

PI3Ks are a family of lipid kinases that phosphorylate the 3-OH of phosphoinositides (Fig. 1).[8–10] Based on their primary

* *Corresponding author:* Tel.: +81 3 3520 0111; fax: +81 3 3570 0484.
E-mail address: yamori@jfcr.or.jp (T. Yamori).
0959-8049/$ - see front matter © 2010 Elsevier Ltd. All rights reserved.
doi:10.1016/j.ejca.2010.01.005

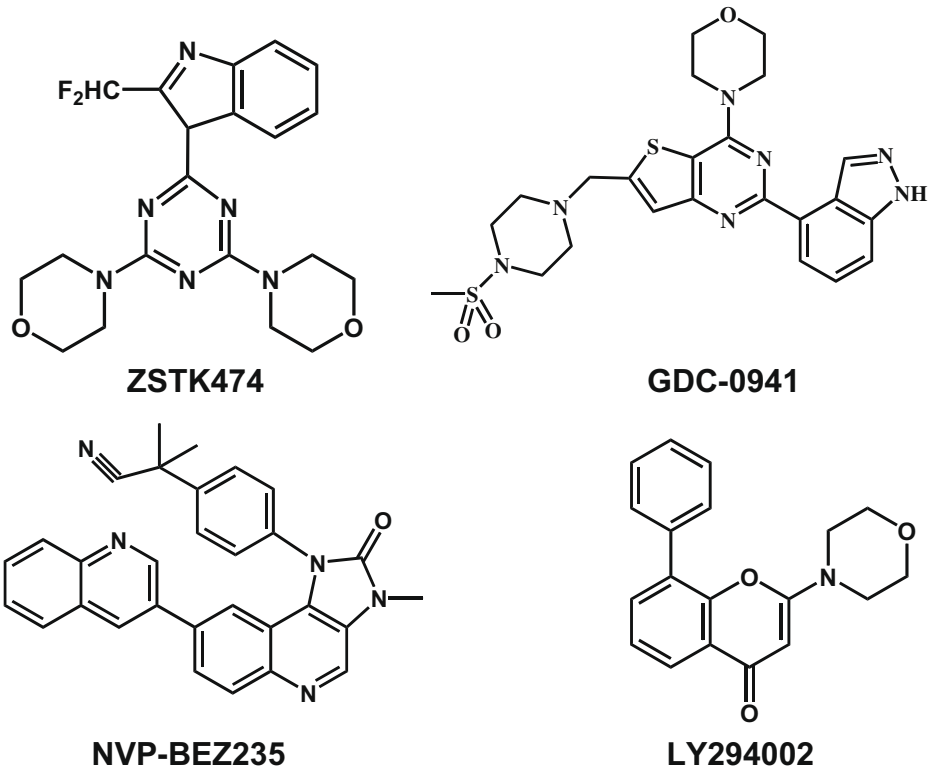

Fig. 1 – Chemical structures of the PI3K inhibitors used in this study.

structures and substrate specificities, PI3Ks are divided into three classes. Class I PI3Ks preferentially phosphorylate phosphatidylinositol 4,5-bisphosphate (PI(4,5)P2) to generate phosphatidylinositol 3,4,5-trisphosphate (PI(3,4,5)P3) (Fig. S1), which plays an important role in cell growth, etc.[11] This class of PI3K is generally referred to as PI3K since much less is known about the functions of other two classes. As a heterodimeric protein, each class I PI3K contains a regulatory subunit (p85 or p101) and a catalytic subunit p110. There are four isoforms of class I PI3Ks, namely PI3Kα, PI3Kβ, PI3Kδ and PI3Kγ, each of which is known to have its own functional role. PI3Kα plays an important role in tumourigenesis since a high frequency of gain-of-function mutations in the PIK3CA gene, which encodes for p110α, has been found in human cancers. [12–14] PI3Kβ is thought to be involved in the development of thrombotic diseases through the activation of platelets.[15] In a recent study, PI3Kβ was shown to play an essential role in tumourigenesis associated with PTEN (phosphatase and tension homologue deleted on chromosome ten) loss or inactivation.[16] Both PI3Kδ and PI3Kγ were reported to be involved in various inflammatory and autoimmune-related diseases.[17–20] Class II PI3Ks contain three members, namely PI3KC2α, PI3KC2β and PI3KC2γ, which phosphorylate phosphatidylinositol (PI) and phosphatidylinositol 4-phosphate (PI(4)P) (Fig. S1). This class of kinases does not require a regulatory subunit to function and is mainly involved in membrane trafficking and receptor internalisation.[21] Class III PI3K contains only one member, namely the vacuolar protein sorting 34 (Vps34), which phosphorylates PI to phosphatidylinositol 3-phosphate (Fig. S1). Vps34 is well known to play important roles in endocytosis and vesicular trafficking.[22–24] Recently, Vps34 was reported to be required for autophagy.[21,25] Phosphatidylinositol 4-kinases (PI4Ks) are a group of lipid kinases that phosphorylate PI to PI(4)P at 4-OH (Fig. S1). Mammalian PI4Ks are now classified into types II and III based on their sensitivities to different inhibitors, because the originally assigned type I PI4Ks were later demonstrated to be PI3K.[26] Amongst these two types of PI4Ks, type III PI4Ks were reported to have structure similar to that of the PI3Ks. By generating PI(4)P, which is the precursor of PI(4,5)P2, PI4Ks play important roles in cell signalling control, etc.[26] PI3K-related protein kinases (PIKKs), which are sometimes called class IV PI3Ks, are protein kinases with similar structure to p110. PIKKs include mammalian target of rapamycin (mTOR) and DNA-dependent protein kinase (DNA-PK), which is known to be involved in protein synthesis or DNA repair.[27] Interestingly, many PI3K inhibitors are also known to inhibit PIKKs.[28,29] In this paper, we have designated three classes of PI3Ks, PI4Ks and PIKKs as the PI3K superfamily.

Since PI3K plays important roles in several diseases, especially in cancer, multiple efforts are being made to develop novel PI3K inhibitors for cancer therapy. While the classical PI3K inhibitors, LY294002 (Fig. 1) and wortmannin, showed *in vivo* antitumour efficacy, both inhibitors failed to enter clinical trials because of their poor solubility or stability,[30] and also because of the associated undesired toxicities.[31,32] However, recent elucidation of the crystal structure of PI3K and its complex with LY294002 [33,34] accelerated the development of new PI3K inhibitors, as a result of which several PI3K inhibitors with antitumour efficacy and low toxicity were obtained. One of these new PI3K inhibitors, PI-103, showed antitumour effects on a variety of tumour types including glioma without

obvious toxicity, but unfavourable pharmacokinetics such as rapid metabolism was observed.[35] As its pharmacologically optimised derivative, GDC-0941 (Fig. 1), showed high oral bioavailability and favourable antitumour effect, and consequently entered phase I clinical trials in 2008.[36,37] Another novel PI3K inhibitor, NVP-BEZ235, (Fig. 1) has exhibited promising antitumour efficacy on various tumour types[29,38,39] and is now undergoing phase I/II clinical trials.[9] In our laboratory, we have recently identified a novel PI3K inhibitor, ZSTK474 (Fig. 1), which exhibited highly promising antitumour efficacy without any obvious toxicity.[6,40]

Even though the above-mentioned novel PI3K inhibitors have all been reported to inhibit class I PI3Ks without revealing any cross-activity to tens of protein kinases,[6,29,37,41] whether they have different molecular targets remained unclear. Since the activities of these inhibitors on the members of PI3K superfamily other than class I PI3K were largely unknown yet, we therefore determined their inhibition profiles for PI3K superfamily and also compared their class I PI3K specificity. Furthermore, we have examined the growth inhibition profiles (fingerprint) of these PI3K inhibitors across JFCR39 panel and compared these fingerprints using the COMPARE analysis programme. Our results indicated that ZSTK474 and GDC-0941 have highly similar inhibition profiles for PI3K superfamily, with higher class I PI3K specificity than NVP-BEZ235 and LY294002. Moreover, ZSTK474 and GDC-0941 showed more similar fingerprints across JFCR39 compared with other two PI3K inhibitors.

2. Materials and methods

2.1. Materials

ZSTK474 was kindly provided by Zenyaku Kogyo Co., Ltd. (Tokyo, Japan). LY294002 and DL-dithiothreitol (DTT) were purchased from Sigma (St. Louis, MO). GDC-0941 was purchased from Symansis (Shanghai, China). NVP-BEZ235 was obtained from Selleck (London ON, Canada). Recombinant PI3Kα, PI3Kβ, PI3Kδ and PI3Kγ, and the PI3K HTRF Assay Kit were purchased from Millipore (Billerica, MA). Recombinant PI3KC2α, PI3KC2β, Vps34, PI4Kβ, mTOR, adenosine 5′-triphosphate disodium salt (ATP), Adapta Universal Kinase Assay Kit, green fluorescent protein labelled 4EBP1 (GFP-4EBP1) and Tb (terbium)-anti-p4EBP1 antibody were purchased from Invitrogen (Carlsbad, CA). DNA-PK, DNA-PK Peptide Substrate and Kinase-Glo Plus Luminescent Kinase Assay Kit were obtained from Promega Corporation (Madison, WI).

2.2. Cell lines

A panel of 39 human cancer cell lines, known as JFCR39, was used as described previously,[1–3] which consists of the following cell lines: lung cancer, NCI-H23, NCI-H226, NCI-H522, NCI-H460, A549, DMS273 and DMS114; colorectal cancer, HCC-2998, KM-12, HT-29, HCT-15 and HCT-116; gastric cancer, MKN-1, MKN-7, MKN-28, MKN-45, MKN-74 and St-4; ovarian cancer, OVCAR-3, OVCAR-4, OVCAR-5, OVCAR-8 and SK-OV-3; breast cancer, BSY-1, HBC-4, HBC-5, MDA-MB-231 and MCF-7; renal cancer, RXF-631L and ACHN; melanoma, LOX-IMVI; glioma, U251, SF-295, SF-539, SF-268, SNB-75 and SNB-78; and prostate cancer, DU-145 and PC-3. All the cell lines were cultured in RPMI 1640 medium supplemented with 5% fetal bovine serum, penicillin (100 U/ml), and streptomycin (100 μg/ml) at 37 °C in humidified air containing 5% CO_2.

2.3. Homogenous time-resolved fluorescence (HTRF) assay for the determination of PI3K activity

The HTRF assay was carried out as described previously.[7] Briefly, various concentrations of the selected inhibitors or DMSO (control) were incubated with the recombinant PI3Kα, PI3Kβ, PI3Kδ and PI3Kγ in the assay buffer supplemented with 10 μM of PI(4,5)P2 in the wells of a 384-well plate at room temperature. The reaction was initiated by the addition of 10 μM ATP and was stopped after 30 min of incubation by adding the stop solution containing EDTA and biotin-PIP3. Detection buffer was then added to each well and the resulting mixture was further incubated for 14 h. Signals from the wells were read using the EnVision 2103 Multilabel Reader (PerkinElmer, Wellesley, MA). The PI3K activity remaining in each well was calculated according to the following formula: PI3K activity (% control) = (sample – minus-enzyme control)/(plus-enzyme control – minus-enzyme control) × 100. For the plus-enzyme control, the kinase was incubated with PI(4,5)P2 and ATP in the absence of the test inhibitor, and for the minus-enzyme control, PI(4,5)P2 was incubated with ATP in the absence of the kinase and the test inhibitor. Representative data from two independent experiments, each carried out in triplicate, were used for plotting. The IC50 values were calculated by fitting the data points to a logistic curve using GraphPad Prism 4 (GraphPad software, San Diego, CA).

2.4. Adapta kinase assay for determining the activities of PI3KC2α, PI3KC2β, Vps34 and PI4Kβ

To determine the activities of PI3KC2α, PI3KC2β, Vps34 and PI4Kβ, a novel non-radioactive assay, known as Adapta kinase assay, was utilised. Adapta kinase assay is a homogenous, fluorescence-based immunoassay, which measures kinase activity in terms of the amount of ADP produced. The assay was performed according to the manufacturer's instructions with minor modifications. The amount of the recombinant kinases were first optimised to keep the reaction velocity within the linear range, and to obtain adequate difference between the resulting signals of the sample in the absence of enzyme and that in the presence of enzyme. Finally, the optimised enzyme concentration (2.0, 7.0, 1.0, and 1.2 μg/ml for PI3KC2α, PI3KC2β, Vps34, and PI4Kβ, respectively) was used to evaluate the inhibitory activities of the test compounds. The kinase reaction and the following ADP detection reaction were carried out in 10 μl volume in a 384-well plate in the kinase reaction buffer containing 20 mM Tris pH 7.5, 5 mM $MgCl_2$, 0.5 mM EGTA, 0.4% Triton X-10 and 2 mM DTT. In the case of Vps34, 2 mM $MnCl_2$ was further added to the assay mixture. In all cases, 2.5 μl of the respective kinase was added and the mixture was incubated at 28 °C in the presence or absence of various concentrations of a given inhibitor. Each reaction was initiated by the addition of 10 μM of ATP and 100 μM of the substrate PI. After incubation for 1 h, 5 μl of the quench/detec-

tion solution containing 10 mM EDTA, 2 nM Eu-labelled anti-ADP antibody, and 20 nM Alexa Fluor 647 ADP tracer, was added to stop the kinase reaction and to detect the formed ADP. After further incubation for 30 min at room temperature, signals from each well were read using Envision 2103 Multilabel Reader in the time-resolved FRET (fluorescence resolved energy transfer) mode. The kinase activity remaining in each well was calculated according to the formula: kinase activity (% control) = (sample – minus-enzyme control)/(plus-enzyme control – minus-enzyme control) × 100. For the plus-enzyme control, each kinase was incubated with its substrate and ATP in the absence of the test inhibitor, and for the minus-enzyme control, the substrate PI was incubated with ATP in the absence of the kinase and the test inhibitor. Representative data from at least two independent experiments, each carried out in triplicate, were used for plotting. The IC50 values were calculated by fitting the data points to a logistic curve using GraphPad Prism 4.

2.5. *LanthaScreen kinase assay for the determination of mTOR activity*

To determine the kinase activity of mTOR in the absence or presence of an inhibitor, another non-radioactive assay, called LanthaScreen Kinase assay, was utilised. Like the Adapta kinase assay described above, LanthaScreen kinase assay is also a homogenous, fluorescence-based time-resolved-FRET immunoassay. With the use of a GFP-labelled mTOR substrate 4EBP1 (GFP-4EBP1), and a Tb-labelled anti-phospho-4EBP1 antibody, this assay measures the activity of mTOR in terms of the amount of phospho-4EBP1 produced. The assay was carried out according to the manufacturer's instructions with minor modifications. To keep the reaction velocity within the linear range and to keep adequate difference between the control (absence of mTOR) and test sample (presence of mTOR) signals, the concentration of the recombinant mTOR was optimised to be 62.5 ng/ml. The assay reaction was carried out in a 384-well plate in 10 μl of kinase reaction buffer consisting of 50 mM HEPES pH 7.5, 0.01% polysobate 20, 1 mM EGTA, 10 mM $MnCl_2$ and 2 mM DTT. First, 2.5 ul of mTOR (62.5 ng/ml) was incubated in the presence or absence of various concentrations of inhibitors (2.5 μl) at 30 °C. Then the reaction was initiated by the addition of 10 μM of ATP and 0.4 μM GFP-4EBP1. After incubation for 1 h at 30 °C, 10 μl of quench/detection solution containing 10 mM EDTA and 2 nM Tb-labelled anti-p4EBP1 antibody, was added to stop the kinase reaction and to detect the phosphorylated 4EBP1. The reaction mixture was then equilibrated for 30 min at room temperature, and the signals from each well were read by using Envision 2103 Multilabel Reader in the time-resolved-FRET mode. The kinase activity of a certain sample was calculated according to the formula: kinase activity (% control) = (sample – minus-enzyme control)/(plus-enzyme control – minus-enzyme control) × 100. For the plus-enzyme control, mTOR was incubated with GFP-4EBP1 and ATP in the absence of the test inhibitor, and for the minus-enzyme control, the substrate was incubated with ATP in the absence of mTOR and the test inhibitor. Representative data from at least two independent experiments, each carried out in triplicate, were used. The IC50 values were calculated by fitting the data points to a logistic curve using GraphPad Prism 4.

2.6. *Kinase-Glo assay for the determination of DNA-PK activity*

DNA-PK activity was determined by using Kinase-Glo assay, a luciferase assay that we previously optimised for assaying the DNA-PK activity.[28] The assay reactions were carried out in a white 96-well plate as described previously.[28] Briefly, DNA-PK was mixed with different concentrations of a test inhibitor, DNA-PK peptide substrate and activation buffer. After pre-incubation for 5 min at 30 °C, ATP was added to initiate the kinase reaction. Next, after 2 h of incubation at 30 °C, the mixture was placed at room temperature for 10 min. Equal volume of Kinase-Glo Assay Plus reagent was then added to initiate the luciferase reaction. Ten minutes later, the luminescence intensity was measured using the EnVision 2103 Multilabel Reader. The DNA-PK activity (% control) of a certain sample was calculated according to the formula: DNA-PK activity (% control) = (sample – minus-enzyme control)/(plus-enzyme control – minus-enzyme control) × 100. For the plus-enzyme control, DNA-PK was incubated with its substrate and ATP in the absence of the test inhibitor, and for the minus-enzyme control, DNA-PK substrate was incubated with ATP in the absence of DNA-PK and the test inhibitor. Representative data from two independent experiments, each carried out in triplicate, were used. The IC50 values were calculated by fitting the data points to a logistic curve using GraphPad Prism 4.

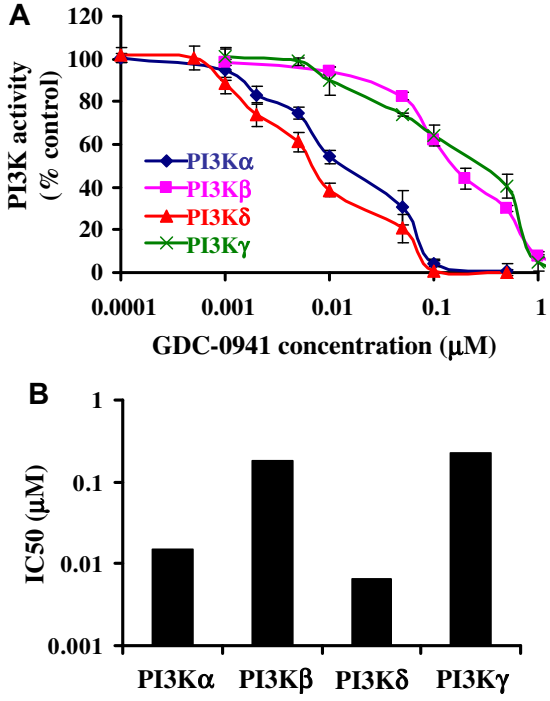

Fig. 2 – Inhibition of class I PI3K isoforms by GDC-0941. (A) Inhibition profiles of GDC-0941 for each class I PI3K isoform. Data shown are mean ± SD (*n* = 3), representative of 2 independent experiments. (B) IC50 values for inhibition of each class I PI3K isoform by GDC-0941.

2.7. Correlation analysis for PI3K superfamily inhibition profiles

The Pearson correlation coefficient (r) between the Log IC50 values of PI3K inhibitors X and Y was calculated using the following formula: $r = (\sum(x_i - x_m)(y_i - y_m))/(\sum(x_i - x_m)^2 \sum(y_i - y_m)^2)^{1/2}$, where x_i and y_i are their respective Log IC50s for each kinase, and x_m and y_m are the mean values of x_i and y_i, respectively ($n = 9$).

2.8. Determination of cell growth inhibition profiles (fingerprint) and COMPARE analysis

Inhibition of cell growth was assessed by the change in total cellular protein following 48 h of treatment with a given compound, and was measured by sulforhodamine B (SRB) assay as described previously.[2,3,42] The concentration of a compound required for 50% growth inhibition (GI50) of cells was calculated as reported.[2,43] The graphic representation (termed

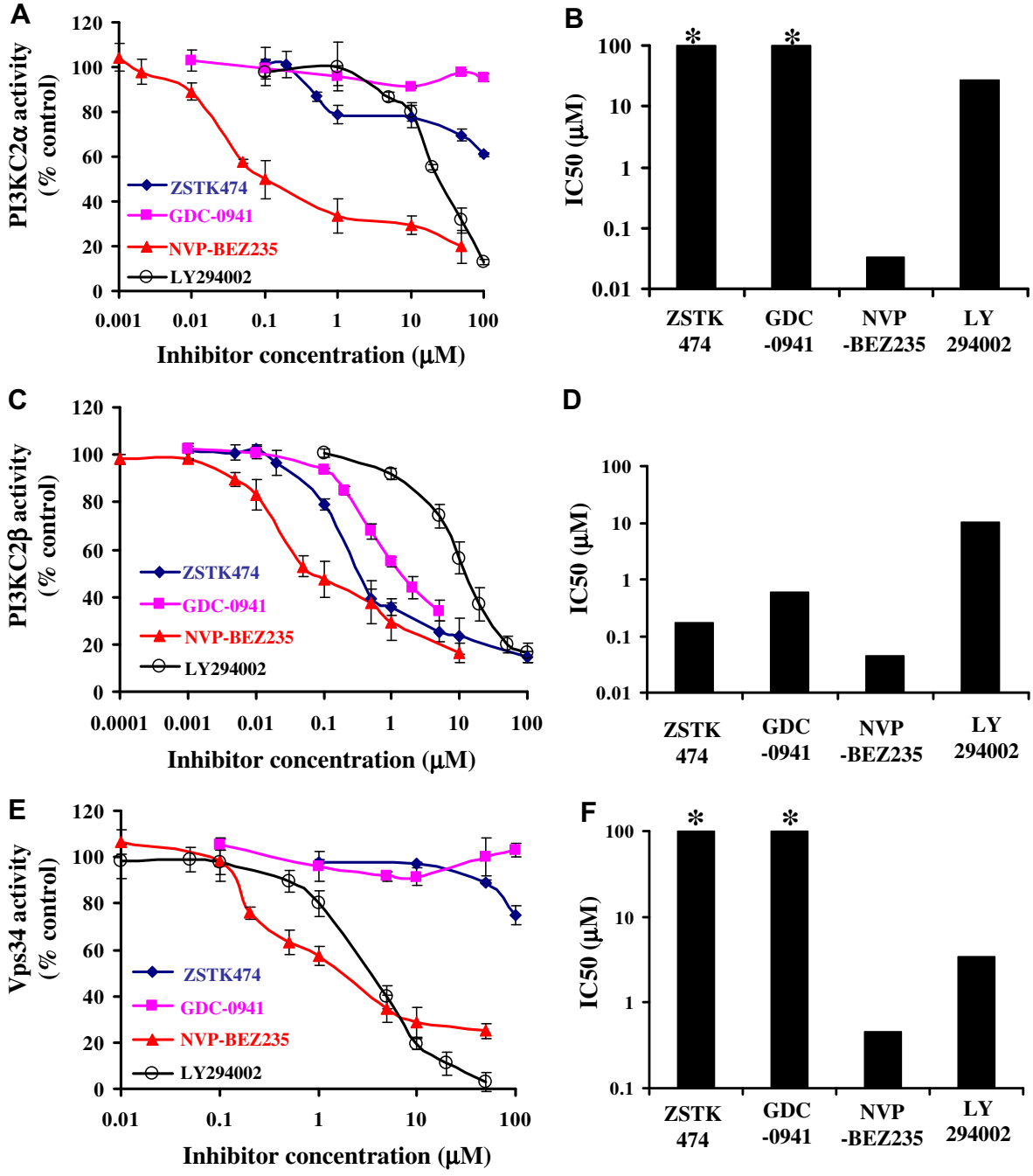

Fig. 3 – Inhibition of class II and III PI3Ks by the selected PI3K inhibitors. Inhibition profiles of the selected PI3K inhibitors for PI3KC2α, PI3KC2β and Vps34 are shown in panels A, C and E, respectively. Data shown are mean ± SD ($n = 3$), representative of 2 or 3 independent experiments. IC50 values of the selected PI3K inhibitors are shown in panels B (PI3KC2α), D (PI3KC2β) and F (Vps34). *: IC50 > 100 μM.

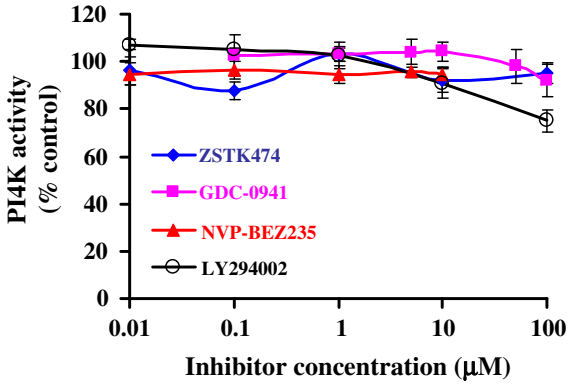

Fig. 4 – Inhibition of PI4K by the selected PI3K inhibitors. Data shown are mean ± SD ($n = 3$), representative of 2 independent experiments.

fingerprint) of a compound's mean differential growth inhibition for the cells used in the JFCR39 panel was plotted based on a calculation that uses a set of GI50 values.[44] At least three independent experiments were carried out, of which the representative fingerprint was used. COMPARE analysis was performed by calculating the Pearson correlation coefficient (r) between the GI50 mean graphs of the compounds X and Y using the following formula: $r = (\sum(x_i - x_m)(y_i - y_m))/(\sum(x_i - x_m)^2 \sum(y_i - y_m)^2)^{1/2}$, where x_i and y_i are Log GI50 of the two compounds, respectively, for each cell line, and x_m and y_m are the mean values of x_i and y_i, respectively ($n = 39$).[2,44] The Pearson correlation coefficients were used to determine the degree of similarity.

3. Results

3.1. GDC-0941 inhibits each class I PI3K isoforms

We previously measured the inhibitory activities of ZSTK474, NVP-BEZ235 and LY294002 against each class I PI3K isoform by HTRF assay, and demonstrated that all of them were pan-class I PI3K isoform inhibitors,[7,28] results of which were consistent with other reports.[29,41] Using the same assay, we have determined the inhibition of each class I PI3K isoform by GDC-0941. As shown in Fig. 2A, GDC-0941 inhibited all the four PI3K isoforms in a dose-dependent manner. The IC50s of GDC-0941 for PI3Kα, PI3Kβ, PI3Kδ and PI3Kγ were found to be 0.015, 0.185, 0.007 and 0.224 μM, respectively (Fig. 2B). Therefore, like the other three selected PI3K inhibitors, GDC-0941 is also a pan-PI3K isoform inhibitor, which was consistent with a recent report.[36]

3.2. Inhibitory activities of ZSTK474, GDC-0941, NVP-BEZ235 and LY294002 against class II and class III PI3Ks

The inhibitory activities of ZSTK474, GDC-0941, NVP-BEZ235 and LY294002, against PI3KC2α, PI3KC2β and Vps34, were

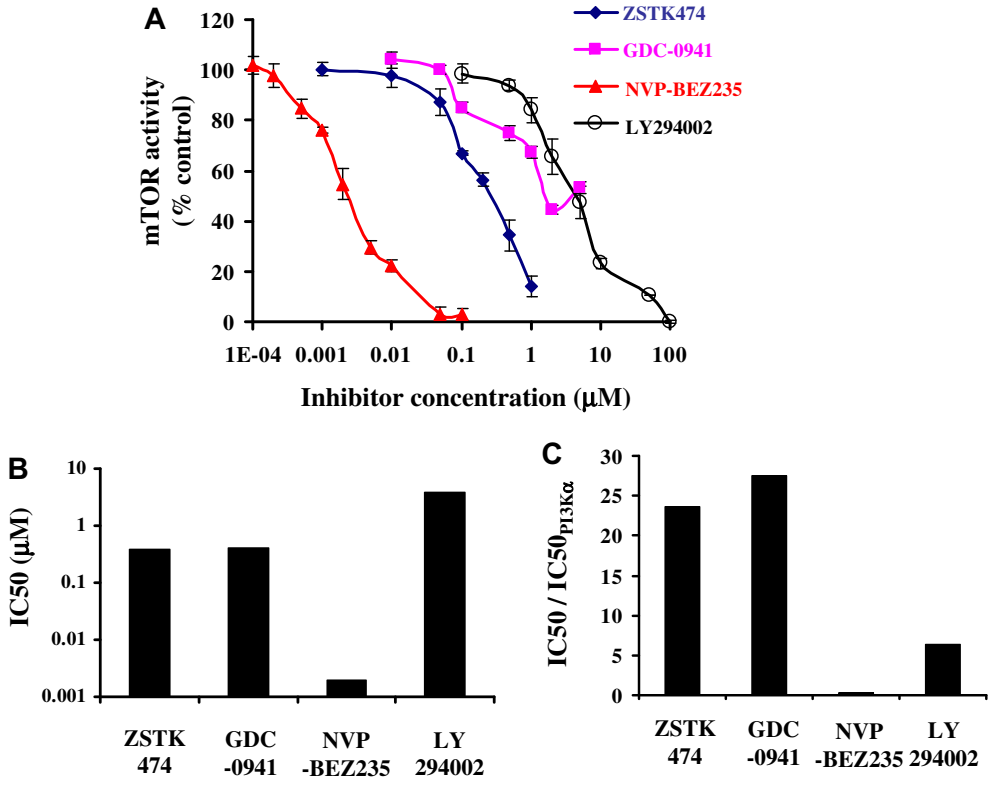

Fig. 5 – ZSTK474 and GDC-0941 selectively inhibit class I PI3K over mTOR. (A) Inhibition profiles of the selected five PI3K inhibitors for mTOR. Data shown are mean ± SD ($n = 3$), representative of 2 or 3 independent experiments. (B) IC50 values of the PI3K inhibitors for mTOR. (C) Selectivity of each PI3K inhibitor for PI3Kα over mTOR. The selectivity index is expressed as the ratio of the IC50 value for mTOR over that for PI3Kα. The IC50 values of ZSTK474, NVP-BEZ235 and LY294002 for PI3Kα are 0.016, 0.007 and 0.6 μM, respectively, as reported previously by us.[7,28]

determined next. Fig. 3A shows various inhibition patterns of the selected PI3K inhibitors. Thus, GDC-0941 did not inhibit PI3KC2α, whereas ZSTK474 only weakly inhibited PI3KC2α even when used at a high concentration of 100 μM. In contrast, both NVP-BEZ235 and LY294002 inhibited PI3KC2α in a dose-dependent manner. The IC50s of them were calculated to be 0.034 and 27.3 μM, respectively (Fig. 3B). With respect to their effect on PI3KC2β, all of the PI3K inhibitors showed inhibitory activity in a dose-dependent manner (Fig. 3C). The IC50s of ZSTK474, GDC-0941, NVP-BEZ235 and LY294002 for PI3KC2β were calculated to be 0.176, 0.590, 0.044 and 10.4 μM, respectively (Fig. 3D). Fig. 3E and F show the inhibition of class III PI3K Vps34 by the selected inhibitors. Similar to the results of PI3KC2α, GDC-0941 did not inhibit Vps34 and ZSTK474 only weakly inhibited Vps34 even when used at 100 μM. The other two inhibitors, NVP-BEZ235 and LY294002 inhibited Vps34 with IC50s of 0.45 and 3.49 μM, respectively.

3.3. *PI4K is not inhibited by any of the selected inhibitors with the exception of LY294002*

Fig. 4 shows the inhibition of PI4K by the indicated concentrations of the selected PI3K inhibitors. As indicated, none of the inhibitors inhibited PI4K, with the exception of LY294002, which inhibited 25% of PI4K at 100 μM.

3.4. *Inhibitory activities of ZSTK474, GDC-0941, NVP-BEZ235 and LY294002 against mTOR*

The inhibition of mTOR by all the selected inhibitors was determined using LanthaScreen assay. As shown in Fig. 5A, all the inhibitors inhibited mTOR in a dose-dependent manner. The IC50 values were calculated and are shown in Fig. 5B. NVP-BEZ235 inhibited mTOR potently, with IC50 value of 0.002 μM. In contrast, ZSTK474, GDC-0941 and LY294002 weakly inhibited mTOR, with IC50 values of 0.377, 0.413 and 3.86 μM, respectively. To further demonstrate their selectivity for class I PI3K, the IC50 values of these inhibitors for mTOR were divided by their corresponding IC50s for class I PI3Kα (0.016, 0.015, 0.007 and 0.6 μM, for ZSTK474, GDC-0941, NVP-BEZ235 and LY294002, respectively), and the resulting ratios were plotted in Fig. 5C. Clearly, ZSTK474 and GDC-0941 revealed much higher selectivity for inhibiting class I PI3K than the other two inhibitors. In contrast, NVP-BEZ235 more potently inhibited the activity of mTOR than that of class I PI3K, suggesting its low class I PI3K inhibition specificity.

3.5. *Inhibition of DNA-PK by GDC-0941*

We have previously measured the inhibitory activities of ZSTK474, NVP-BEZ235 and LY294002 against DNA-PK, by

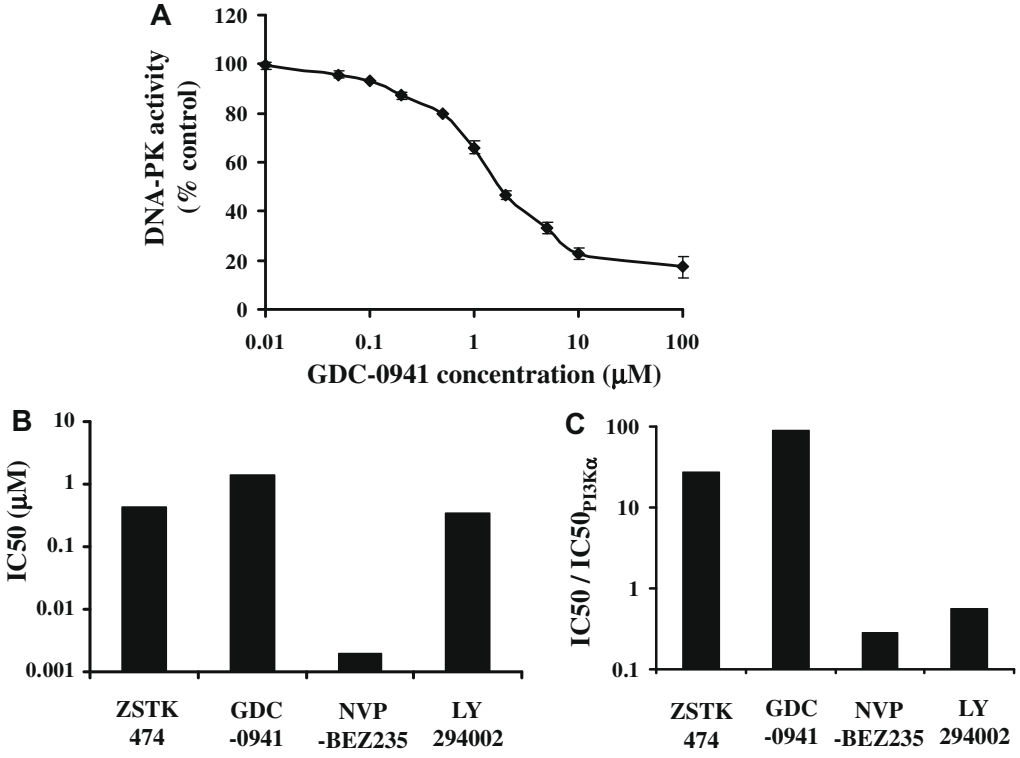

Fig. 6 – ZSTK474 and GDC-0941 selectively inhibit class I PI3K over DNA-PK. (A) Inhibition profile of GDC-0941 for DNA-PK. Data shown are mean ± SD (n = 3), representative of 2 independent experiments. (B) IC50 values of the four PI3K inhibitors for DNA-PK. IC50 values of ZSTK474, NVP-BEZ235 and LY294002 for DNA-PK are 0.436, 0.002 and 0.335 μM, respectively, as reported previously by us. (C) Selectivity of each PI3K inhibitor for PI3Kα over DNA-PK. The selectivity index is expressed as the ratio of the IC50 value for DNA-PK over that for PI3Kα. The IC50 values of ZSTK474, NVP-BEZ235 and LY294002 for PI3Kα are 0.016, 0.007 and 0.6 μM, respectively.[7,28]

using Kinase-Glo assay we established.[28] Here, we determined the activity of GDC-0941 against DNA-PK by the same assay. As shown in Fig 6A, GDC-0941 inhibited DNA-PK in a dose-dependent manner. The IC50 was calculated to be 1.37 μM. This IC50 value of GDC-0941 and those values of the other three inhibitors determined previously by us[28] were plotted in Fig. 6B, and were used to determine the specificities for class I PI3K shown in Fig. 6C. Like ZSTK474, GDC-0941 revealed much higher specificity for inhibiting class I PI3K than NVP-BEZ235 and LY294002.

3.6. ZSTK474 and GDC-0941 indicate highly similar inhibition profiles for PI3K superfamily

IC50 plots for inhibiting the representative members of PI3K superfamily are shown in Fig. 7A (for ZSTK474 and GDC-0941) and Fig. S2 (for NVP-BEZ235 and LY294002). As indicated, the inhibition pattern of ZSTK474 was highly similar to that of GDC-0941, and both significantly differed from the inhibition patterns of the other two inhibitors (Fig. 7A and Fig. S2). To further confirm the similarities between the inhibition patterns of ZSTK474 and GDC-0941, correlation analysis was carried out using their respective Log IC50 values and the result is shown in Fig. 7B. From this plot, the correlation coefficient was determined to be 0.985, which further confirmed that ZSTK474 and GDC-0941 inhibited PI3K superfamily in a highly similar fashion.

3.7. ZSTK474 and GDC-0941 have similar JFCR39 GI50 fingerprints

ZSTK474 was originally identified as a PI3K inhibitor by comparison of its JFCR39 fingerprint with that of LY294002.[6] Here, we have determined the cell growth inhibition profiles of GDC-0941, NVP-BEZ235, together with ZSTK474 and LY294002, and obtained their fingerprints for the JFCR39 panel (Figs. 8 and S3). ZSTK474 and GDC-0941 exhibited similar fingerprints, suggesting the similarity between their cell growth inhibition profiles across the JFCR39 panel. Furthermore, using ZSTK474 as a seed, we carried out COMPARE analysis of the PI3K inhibitors together with 8 anticancer drugs including topoisomerase inhibitors SN-38, Topotecan, Amsacrine and Etoposide, antimetabolites 1-hexylcarbamoyl-5-fluorouracil (HCFU), 5-fluorouracil (5-FU), and tubulin binders Docetaxel and Paclitaxel. As a result, the other three PI3K inhibitors showed much higher similarity with ZSTK474 ($r \geqslant 0.670$), compared with the 8 anticancer drugs ($r \leqslant 0.201$), due to the fact that all the PI3K inhibitors share a common class I PI3K target with ZSTK474 (Table 1). Amongst the three PI3K inhibitors, GDC-0941 exhibited a correlation coefficient value of 0.863, higher than NVP-BEZ235 and LY294002, in similarity with ZSTK474. This result suggests that ZSTK474 shares more in the molecular targets with GDC-0941 than with either of the other two PI3K inhibitors, consistent with the result obtained from the biochemical assay. In addition, we also carried out COMPARE analysis by using Etoposide,

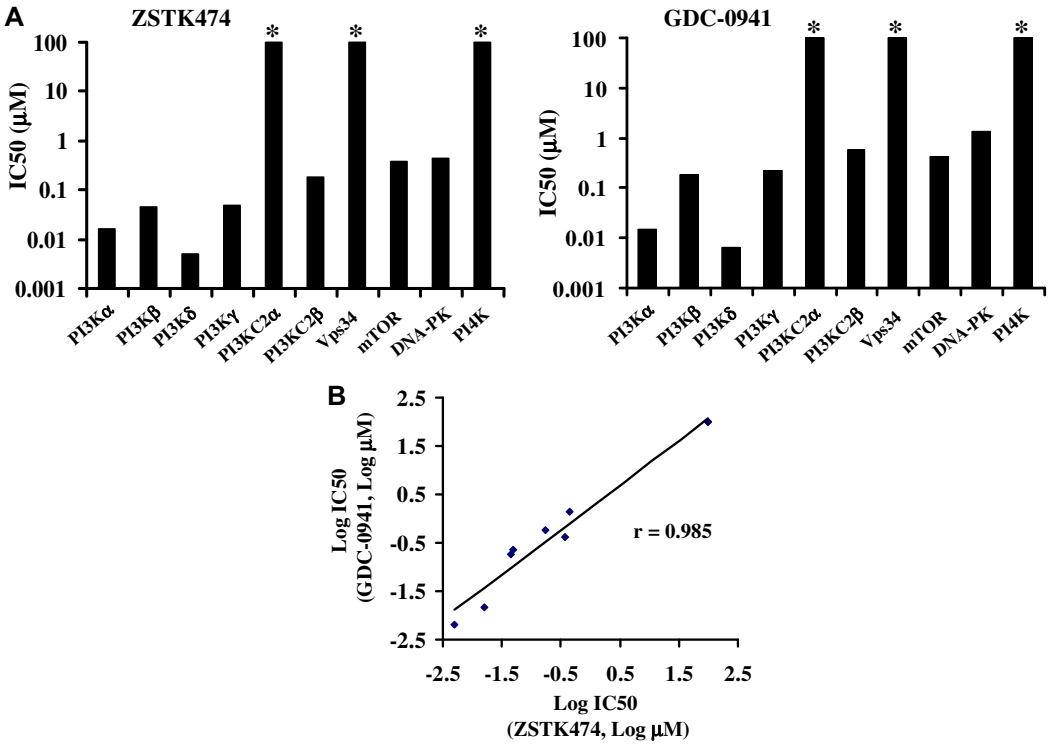

Fig. 7 – High similarity between the inhibition patterns of ZSTK474 and GDC-0941 for PI3K superfamily. (A) IC50 plots of ZSTK474 and GDC-0941 for inhibiting PI3K superfamily. *: IC50 > 100 μM. (B) Pearson correlation analysis shows a linear relationship between the log IC50 values of ZSTK474 and GDC-0941, suggesting high similarity between the inhibition patterns of ZSTK474 and GDC-0941 for PI3K superfamily. *r*: Pearson correlation coefficient.

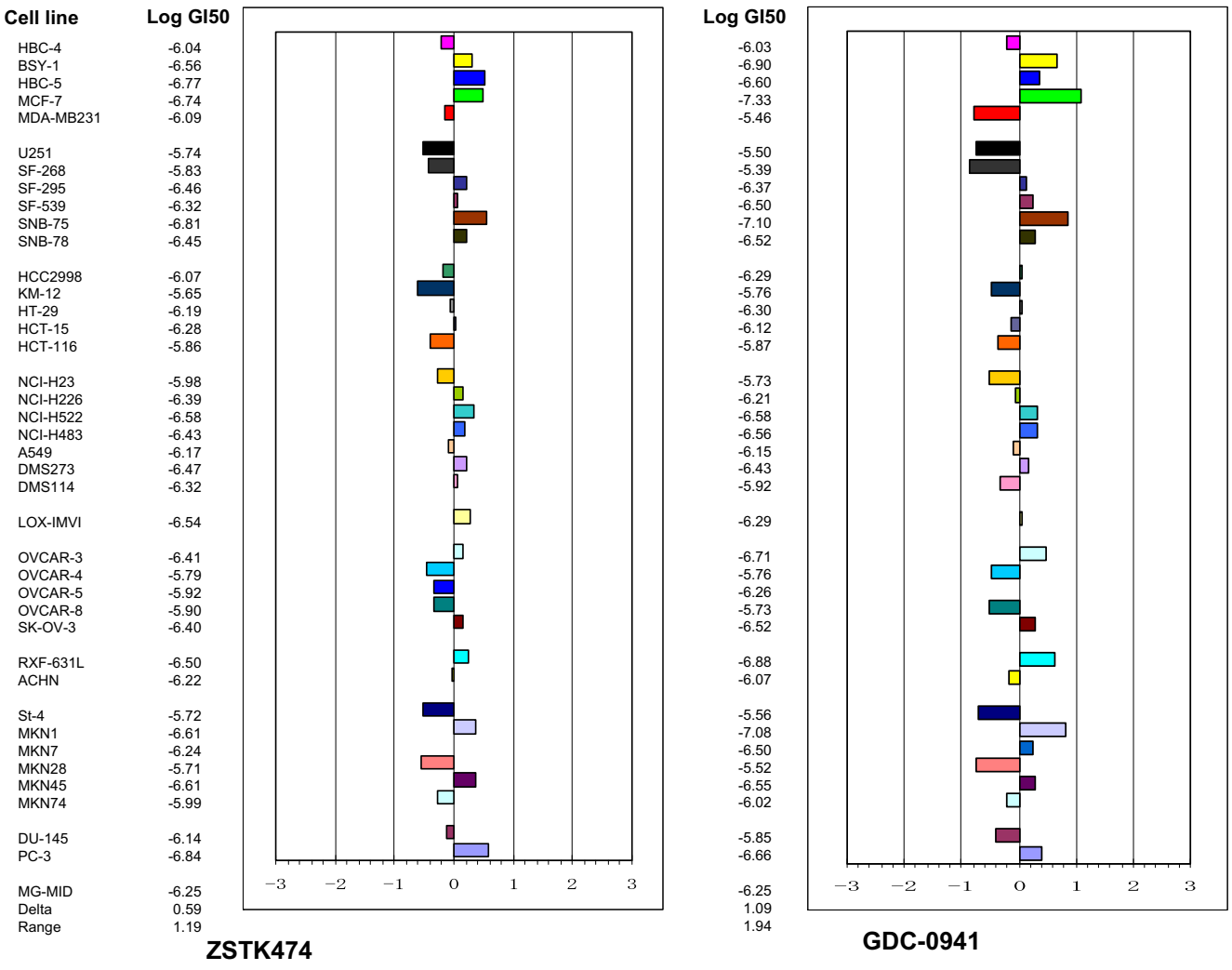

Fig. 8 – High similarity between the JFCR39 fingerprints of ZSTK474 and GDC-0941. JFCR39 fingerprints of ZSTK474 and GDC-0941 are shown. Fingerprint indicates the differential growth inhibition pattern of ZSTK474 or GDC-0941 for the cell lines in JFCR39 panel. The X-axis shows difference in logarithmic scale between the mean of Log GI50 values for all 39 cell lines (MG-MID, expressed as 0 in the fingerprint) and the Log GI50 for each cell line in JFCR39 panel. Columns to the right of 0 indicate the sensitivity of the cell lines to a given compound and columns to the left indicate the resistance. MG-MID = mean of Log GI50 values for all 39 cell lines; Delta = difference between the MG-MID and the Log GI50 value for the most sensitive cell line; Range = difference between the Log GI50 values for the most resistant cell line and the most sensitive cell line.

Table 1 – COMPARE analysis with ZSTK474 as a seed.

Rank	Compound	Correlation coefficient (*r*)
1	GDC-0941	0.863
2	LY294002	0.749
3	NVP-BEZ235	0.67
4	Amsacrine	0.201
5	Etoposide	0.192
6	Topotecan	0.189
7	Docetaxel	0.159
8	SN-38	0.13
9	HCFU	0.082
10	Paclitaxel	0.061
11	5-FU	−0.068

Paclitaxel and 5-FU as seeds, respectively. The results showed that compounds with the same molecular target (Amsacrine, SN-38 and Topotecan for Etoposide; Docetaxel for Paclitaxel; HCFU for 5-FU) exhibit high correlation coefficient, demonstrating that JFCR39 is reliable for molecular target identification (data not shown).

4. Discussion

In this study, biochemical assay of the activities of the selected PI3K inhibitors on PI3K superfamily demonstrated that ZSTK474 had a similar inhibition pattern with GDC-0941; COMPARE analysis of their inhibition profiles against JFCR39 also indicated that they have highly similar fingerprints, thus suggesting the existence of highly overlapping molecular targets between them.

JFCR39 was established in the early 1990s by exploiting the methods and some of the tumour cell lines used in NCI60,

supplemented with other cell lines of particular interest in Japan.[45] We previously demonstrated that JFCR39 could be utilised for molecular target identification. The present study further suggests that JFCR39 is able to provide valuable information regarding the molecular target specificity of a PI3K inhibitor with respect to its activity against PI3K superfamily, and thus, provides further support to the idea that this information-rich system could be used as a reliable approach for molecular target identification.

In addition to predicting the molecular target or action mechanism of an agent, JFCR39 could also provide information on disease-oriented cancer chemotherapy, since the fingerprint reflects the sensitivity of each individual cancer cell line. For example, prostate cancer cell PC-3 exhibits comparatively higher sensitivity to all the PI3K inhibitors used in this study (Fig. 8 and Fig. S3), suggesting that PI3K inhibitor could be expected to treat patients with such tumour type when approved. The relatively higher sensitivity of PC-3 cell to PI3K inhibitors could be explained by loss of function of PTEN, the counterpart of PI3K, in this cell.[46] In contrast, lung cancer cell NCI-H23 shows relative resistance to all PI3K inhibitors (Fig. 8 and Fig. S3), which might be attributed to the K-RAS mutation in this cell.[47]

ZSTK474 and GDC-0941 indicated no or weak inhibition against class II and class III PI3Ks, PI4K, mTOR and DNA-PK, suggesting that both of them are specific class I PI3K inhibitors. In contrast, NVP-BEZ235 seems to be a non-specific class I PI3K inhibitor, because it inhibited the activities of mTOR, DNA-PK and class II PI3Ks with higher or similar potencies, compared with that of class I PI3Ks. This study is the first report describing the inhibitory activities of these inhibitors against class II and class III PI3Ks and PI4K.

GDC-0941 and NVP-BEZ235 are presently undergoing clinical trials. Even though both of them did not inhibit dozens of protein kinases,[29,37] our results revealed that they inhibited members of PI3K superfamily with different selectivity. GDC-0941 was shown to be a specific class I PI3K inhibitor while NVP-BEZ235 exhibited similar potency on mTOR and DNA-PK to that on class I PI3K. Dual targeting both class I PI3K and mTOR was reported to enhance the antitumour activity *in vitro*.[38] On the other hand, additional inhibition of DNA-PK might lead to side-effect.[48] However, the available *in vivo* data showed that GDC-0941 exhibited potent efficacy on U87MG and other xenografts,[37,49] and NVP-BEZ235 was also well tolerated without obvious toxicity.[29,39] Therefore, whether the difference in class I PI3K specificity affect the therapeutic efficacy and/or side-effects remains unclear at present. An answer to this question would have to wait for the results of the ongoing clinical trials.

Like GDC-0941, ZSTK474 inhibited class I PI3K but not Vps34. Recently, it was reported that class I and class III PI3K play opposite roles in autophagy.[50] By producing PI(3,4,5)P3 and activating the downstream mTOR, class I PI3K inhibits autophagy.[51] In contrast, Vps34 promotes autophagy by forming a multiprotein complex with Beclin 1, etc.[25,50] Therefore, based on their differential effects on class I and class III PI3Ks, ZSTK474 and GDC-0941 are expected to induce autophagy. Our preliminary results indicate that ZSTK474 could indeed induce autophagy (data not shown). Detailed investigations are ongoing.

5. Conflict of interest statement

Takao Yamori has a research fund from Zenyaku Kogyo Co., Ltd., which is the proprietary company of ZSTK474. No conflict of interest is declared for the other authors.

Acknowledgements

We thank Dr. R.H. Shoemaker and Dr. K.D. Paull for discussion on the establishment of JFCR39 anticancer drug screening system; and also thank Ms. Y. Nishimura, Ms. M. Seki, Ms. Y. Mukai, Ms. M. Okamura and Ms. Y. Ohashi for their assistance in the determination of cell growth inhibition. ZSTK474 was kindly provided by Zenyaku Kogyo Co., Ltd. This work was supported by a grant from the National Institute of Biomedical Innovation, Japan to T. Yamori (05-13); a grants-in-aid of the Priority Area "Cancer" from the Ministry of Education, Culture, Sports, Science, and Technology of Japan to T. Yamori (20015048); a grants-in-aid for Scientific Research (B) from Japan Society for the Promotion of Science to T. Yamori (17390032); and a grant from Kobayashi institute for innovative cancer chemotherapy.

Appendix A. Supplementary data

Supplementary data associated with this article can be found, in the online version, at doi:10.1016/j.ejca.2010.01.005.

REFERENCES

1. Yamori T. Panel of human cancer cell lines provides valuable database for drug discovery and bioinformatics. *Cancer Chemother Pharmacol* 2003;**52**(Suppl. 1):S74–9.
2. Yamori T, Matsunaga A, Sato S, et al. Potent antitumor activity of MS-247, a novel DNA minor groove binder, evaluated by an in vitro and in vivo human cancer cell line panel. *Cancer Res* 1999;**59**:4042–9.
3. Nakatsu N, Nakamura T, Yamazaki K, et al. Evaluation of action mechanisms of toxic chemicals using JFCR39, a panel of human cancer cell lines. *Mol Pharmacol* 2007;**72**:1171–80.
4. Dan S, Tsunoda T, Kitahara O, et al. An integrated database of chemosensitivity to 55 anticancer drugs and gene expression profiles of 39 human cancer cell lines. *Cancer Res* 2002;**62**:1139–47.
5. Naasani I, Seimiya H, Yamori T, et al. FJ5002: a potent telomerase inhibitor identified by exploiting the disease-oriented screening program with COMPARE analysis. *Cancer Res* 1999;**59**:4004–11.
6. Yaguchi S, Fukui Y, Koshimizu I, et al. Antitumor activity of ZSTK474, a new phosphatidylinositol 3-kinase inhibitor. *J Natl Cancer Inst* 2006;**98**:545–56.
7. Kong D, Yamori T. ZSTK474 is an ATP-competitive inhibitor of class I phosphatidylinositol 3 kinase isoforms. *Cancer Sci* 2007;**98**:1638–42.
8. Kong D, Yamori T. Phosphatidylinositol 3-kinase inhibitors: promising drug candidates for cancer therapy. *Cancer Sci* 2008;**99**:1734–40.
9. Kong D, Yamori T. Advances in development of phosphatidylinositol 3-kinase inhibitors. *Curr Med Chem* 2009;**16**:2839–54.

10. Toker A, Cantley LC. Signalling through the lipid products of phosphoinositide-3-OH kinase. *Nature* 1997;**387**:673–6.
11. Franke TF, Kaplan DR, Cantley LC. PI3K: downstream AKTion blocks apoptosis. *Cell* 1997;**88**:435–7.
12. Levine DA, Bogomolniy F, Yee CJ, et al. Frequent mutation of the PIK3CA gene in ovarian and breast cancers. *Clin Cancer Res* 2005;**11**:2875–8.
13. Samuels Y, Wang Z, Bardelli A, et al. High frequency of mutations of the PIK3CA gene in human cancers. *Science* 2004;**304**:554.
14. Whyte DB, Holbeck SL. Correlation of PIK3Ca mutations with gene expression and drug sensitivity in NCI-60 cell lines. *Biochem Biophys Res Commun* 2006;**340**:469–75.
15. Jackson SP, Schoenwaelder SM, Goncalves I, et al. PI 3-kinase p110beta: a new target for antithrombotic therapy. *Nat Med* 2005;**11**:507–14.
16. Jia S, Liu Z, Zhang S, et al. Essential roles of PI(3)K-p110beta in cell growth, metabolism and tumorigenesis. *Nature* 2008;**454**:776–9.
17. Sadhu C, Masinovsky B, Dick K, et al. Essential role of phosphoinositide 3-kinase delta in neutrophil directional movement. *J Immunol* 2003;**170**:2647–54.
18. Sasaki T, Irie-Sasaki J, Jones RG, et al. Function of PI3Kgamma in thymocyte development, T cell activation, and neutrophil migration. *Science* 2000;**287**:1040–6.
19. Barber DF, Bartolome A, Hernandez C, et al. PI3Kgamma inhibition blocks glomerulonephritis and extends lifespan in a mouse model of systemic lupus. *Nat Med* 2005;**11**:933–5.
20. Camps M, Ruckle T, Ji H, et al. Blockade of PI3Kgamma suppresses joint inflammation and damage in mouse models of rheumatoid arthritis. *Nat Med* 2005;**11**:936–43.
21. Carracedo A, Pandolfi PP. The PTEN-PI3K pathway: of feedbacks and cross-talks. *Oncogene* 2008;**27**:5527–41.
22. Murray JT, Panaretou C, Stenmark H, et al. Role of Rab5 in the recruitment of hVps34/p150 to the early endosome. *Traffic* 2002;**3**:416–27.
23. Christoforidis S, Miaczynska M, Ashman K, et al. Phosphatidylinositol-3-OH kinases are Rab5 effectors. *Nat Cell Biol* 1999;**1**:249–52.
24. Backer JM. The regulation and function of Class III PI3Ks: novel roles for Vps34. *Biochem J* 2008;**410**:1–17.
25. Juhasz G, Hill JH, Yan Y, et al. The class III PI(3)K Vps34 promotes autophagy and endocytosis but not TOR signaling in Drosophila. *J Cell Biol* 2008;**181**:655–66.
26. D'Angelo G, Vicinanza M, Di Campli A, et al. The multiple roles of PtdIns(4)P – not just the precursor of PtdIns(4,5)P2. *J Cell Sci* 2008;**121**:1955–63.
27. Marone R, Cmiljanovic V, Giese B, et al. Targeting phosphoinositide 3-kinase: moving towards therapy. *Biochim Biophys Acta* 2008;**1784**:159–85.
28. Kong D, Yaguchi S, Yamori T. Effect of ZSTK474, a novel phosphatidylinositol 3-kinase inhibitor, on DNA-dependent protein kinase. *Biol Pharm Bull* 2009;**32**:297–300.
29. Maira SM, Stauffer F, Brueggen J, et al. Identification and characterization of NVP-BEZ235, a new orally available dual phosphatidylinositol 3-kinase/mammalian target of rapamycin inhibitor with potent in vivo antitumor activity. *Mol Cancer Ther* 2008;**7**:1851–63.
30. Garlich JR, De P, Dey N, et al. A vascular targeted pan phosphoinositide 3-kinase inhibitor prodrug, SF1126, with antitumor and antiangiogenic activity. *Cancer Res* 2008;**68**:206–15.
31. Hu L, Zaloudek C, Mills GB, et al. In vivo and in vitro ovarian carcinoma growth inhibition by a phosphatidylinositol 3-kinase inhibitor (LY294002). *Clin Cancer Res* 2000;**6**:880–6.
32. Ihle NT, Williams R, Chow S, et al. Molecular pharmacology and antitumor activity of PX-866, a novel inhibitor of phosphoinositide-3-kinase signaling. *Mol Cancer Ther* 2004;**3**:763–72.
33. Walker EH, Pacold ME, Perisic O, et al. Structural determinants of phosphoinositide 3-kinase inhibition by wortmannin, LY294002, quercetin, myricetin, and staurosporine. *Mol Cell* 2000;**6**:909–19.
34. Walker EH, Perisic O, Ried C, et al. Structural insights into phosphoinositide 3-kinase catalysis and signalling. *Nature* 1999;**402**:313–20.
35. Fan QW, Knight ZA, Goldenberg DD, et al. A dual PI3 kinase/mTOR inhibitor reveals emergent efficacy in glioma. *Cancer Cell* 2006;**9**:341–9.
36. Raynaud FI, Eccles SA, Patel S, et al. Biological properties of potent inhibitors of class I phosphatidylinositide 3-kinases: from PI-103 through PI-540, PI-620 to the oral agent GDC-0941. *Mol Cancer Ther* 2009;**8**:1725–38.
37. Folkes AJ, Ahmadi K, Alderton WK, et al. The identification of 2-(1H-indazol-4-yl)-6-(4-methanesulfonyl-piperazin-1-ylmethyl)-4-morpholin-4-yl-thieno3,2-dpyrimidine (GDC-0941) as a potent, selective, orally bioavailable inhibitor of class I PI3 kinase for the treatment of cancer. *J Med Chem* 2008;**51**:5522–32.
38. Marone R, Erhart D, Mertz AC, et al. Targeting melanoma with dual phosphoinositide 3-kinase/mammalian target of rapamycin inhibitors. *Mol Cancer Res* 2009;**7**:601–13.
39. McMillin DW, Ooi M, Delmore J, et al. Antimyeloma activity of the orally bioavailable dual phosphatidylinositol 3-kinase/mammalian target of rapamycin inhibitor NVP-BEZ235. *Cancer Res* 2009;**69**:5835–42.
40. Kong D, Okamura M, Yoshimi H, et al. Antiangiogenic effect of ZSTK474, a novel phosphatidylinositol 3-kinase inhibitor. *Eur J Cancer* 2009;**45**:857–65.
41. Raynaud FI, Eccles S, Clarke PA, et al. Pharmacologic characterization of a potent inhibitor of class I phosphatidylinositide 3-kinases. *Cancer Res* 2007;**67**:5840–50.
42. Skehan P, Storeng R, Scudiero D, et al. New colorimetric cytotoxicity assay for anticancer-drug screening. *J Natl Cancer Inst* 1990;**82**:1107–12.
43. Monks A, Scudiero D, Skehan P, et al. Feasibility of a high-flux anticancer drug screen using a diverse panel of cultured human tumor cell lines. *J Natl Cancer Inst* 1991;**83**:757–66.
44. Paull KD, Shoemaker RH, Hodes L, et al. Display and analysis of patterns of differential activity of drugs against human tumor cell lines: development of mean graph and COMPARE algorithm. *J Natl Cancer Inst* 1989;**81**:1088–92.
45. Shoemaker RH. The NCI60 human tumour cell line anticancer drug screen. *Nat Rev Cancer* 2006;**6**:813–23.
46. Fang J, Ding M, Yang L, et al. PI3K/PTEN/AKT signaling regulates prostate tumor angiogenesis. *Cell Signal* 2007;**19**:2487–97.
47. Mitsudomi T, Viallet J, Mulshine JL, et al. Mutations of ras genes distinguish a subset of non-small-cell lung cancer cell lines from small-cell lung cancer cell lines. *Oncogene* 1991;**6**:1353–62.
48. Carnero A. Novel inhibitors of the PI3K family. *Expert Opin Investig Drugs* 2009;**18**:1265–77.
49. Junttila TT, Akita RW, Parsons K, et al. Ligand-independent HER2/HER3/PI3K complex is disrupted by trastuzumab and is effectively inhibited by the PI3K inhibitor GDC-0941. *Cancer Cell* 2009;**15**:429–40.
50. Petiot A, Ogier-Denis E, Blommaart EF, et al. Distinct classes of phosphatidylinositol 3′-kinases are involved in signaling pathways that control macroautophagy in HT-29 cells. *J Biol Chem* 2000;**275**:992–8.
51. Moretti L, Yang ES, Kim KW, et al. Autophagy signaling in cancer and its potential as novel target to improve anticancer therapy. *Drug Resist Updat* 2007;**10**:135–43.